EXPERIMENTAL VERIFICATION OF MATHEMATICAL MODEL OF THE HEAT TRANSFER IN EXHAUST SYSTEM

by

Snežana PETKOVIĆ, Radivoje PEŠIĆ, Jovanka LUKIĆ

Original scientific paper
UDC:
DOI:

A Catalyst convertor has maximal efficiency when it reaches working temperature. In a cold start phase efficiency of the catalyst is low and exhaust emissions have high level of air pollutants. The exhaust system optimization, in order to decrease time of achievement of the catalyst working temperature, caused reduction of the total vehicle emission. Implementation of mathematical models in development of exhaust systems decrease total costs and reduce time. Mathematical model has to be experimentally verified and calibrated, in order to be useful in the optimization process. Measurement installations have been developed and used for verification of the mathematical model of unsteady heat transfer in exhaust systems. Comparisons between experimental results and the mathematical model are presented in this paper. Based on obtained results, it can be concluded that there is a good agreement between the model and the experimental results.

Key words*: Cold start phase, Exhaust system, heat transfer, experimental verification, mathematical model*

1. Introduction

The objective of the modern society is to make new relations between humans and automobiles, based on harmony with the global environment. The first step in this direction is the introduction of legal limits on exhaust emissions of automobiles. With the sequence of new technological solutions, the exhaust emissions of the vehicles are reduced by 98% in relation to the level achieved before the regulations on exhaust emission were introduced. Such efficiency in reducing the exhaust emission can only be achieved when the catalyst has reached the working temperature. The warming-up period of the engine and the catalyst is usually called CSP *(Cold Start Phase)* [1]. Literature data show that approximately 60-80% of total vehicle emission of HC *(Hydro Carbon)* and CO *(Carbon Oxide)*, during CSP at environmental air temperature of 18 °C, is emitted in the warming-up period. Between 95% and 98% of total vehicle emissions are released during the warming-up period at environmental air temperature below 0 °C, [2, 3].

The main quantity of the real time NO (*Nitrogen Oxide*) emissions are released in the first several cycles during the cold start. The NO emissions decrease gradually in the following cycle. Because of the unfavourable combustion conditions during the cold start phase, the richer mixture

concentration is used in the first several cycles in order to ensure successful combustion. At that time, the cylinder pressure and combustion temperature increase sharply, giving rise to increased NO emissions [4].

There are also high particle emissions after cold start of a Diesel engine [5].

Emission reduction during CSP significantly contributes to total vehicle emission reduction. The present authors developed a one-dimensional mathematical model of unsteady heating-up of the exhaust system parts (manifold, pipes and catalyst) during CSP, in order to make a contribution to solving the problem of increased vehicle emission [6, 7]. Verification and calibration of the model with results of experimental research are necessary for further model application. The measurement installations for validation of the mathematical models are developed.

Results of conducted experimental research will be presented in the paper. Successful verification and validation of the mathematical model of warming-up of the exhaust system will produce conditions for the model application in optimization process of the exhaust system to give the shortest time of the catalyst warming-up.

2. Mathematical model

The present authors have previously developed a one-dimensional mathematical model of unsteady heating-up of the exhaust system parts (the exhaust manifold, the exhaust pipes and the catalyst). Detailed description of the model can be found in the papers [6, 7]. A short description of that model will be shown in this chapter for convenience.

2.1. Heat transfer in the exhaust pipe

In developing the model of heat transfer in the exhaust pipe the following assumptions were taken into account:

- A quasi-steady incompressible flow,
- During small calculation time step (Δt), and in an infinitesimal control gas volume ($\Delta V_g = V_1 = D_1^2 \pi/4 \cdot \Delta x$), the gas temperature is assumed to be constant, ($\frac{\partial T_g}{\partial t} = 0$),
- The gas pressure in exhaust system has a small change,
- The gas density depend only on the gas temperature,
- Heat conduction through the gas in the axial direction is neglected, ($\frac{\partial^2 T_g}{\partial x^2} = 0$),
- For an infinitesimal control volume of the pipe wall ($\Delta V_m = V_2 - V_1 = (D_2^2 - D_1^2)\pi/4 \cdot \Delta x$) a uniform temperature distribution within the small calculation time step (T_m = const.) is assumed, and
- The radial temperature gradient in the exhaust pipe wall is neglected (due to a small exhaust pipe wall thickness and high heat conductivity of metal).

Based on the aforementioned assumptions and taking into account the convective heat transfer between the exhaust gas and the pipe wall, heat losses into the environment by convection and radiation, one-dimensional energy equations for the exhaust gas and the exhaust pipe wall can be written as:

$$\rho_g \cdot c_{pg} \cdot u \cdot \frac{\partial T_g}{\partial x} = \dot{q}_{gen} = -\frac{\alpha_{cvu} \cdot \pi \cdot D_1 \cdot \Delta x \cdot (T_g - T_m)}{\Delta V_g} \quad (1)$$

$$\frac{\partial T_g}{\partial x} = -\frac{\alpha_{cvu} \cdot \pi \cdot D_1 \cdot (T_g - T_m)}{\rho_g \cdot u \cdot \Delta V_g / \Delta x \cdot c_{pg}} = -\frac{\alpha_{cvu} \cdot \pi \cdot D_1 \cdot (T_g - T_m)}{\dot{m}_g \cdot c_{pg}}$$

$$\frac{\partial T_m}{\partial t} = a_m \frac{\partial^2 T_m}{\partial x^2} + \frac{\delta \dot{Q}_{cvu} - \delta \dot{Q}_{cvo} - \delta \dot{Q}_{rado}}{\rho_m \cdot c_m \cdot \Delta V_m} \quad (2)$$

where:

T_g – Gas temperature, [K],
T_m – Pipe wall temperature, [K],
ρ_g – Mass density of the gas, [kg/m^3],
c_{pg} – Specific heat of the gas at constant pressure, [J·kg^{-1}·K^{-1}],
a_m – Thermal diffusivity of the material (pipe wall), ($=\lambda_m/\rho_m/c_m$), [m^2·s^{-1}].
ρ_m – Mass density of the pipe, [kg/m^3],
c_m – Specific heat of the pipe, [J·kg^{-1}·K^{-1}],
λ_m – Thermal conductivity of the pipe, [W·m^{-1}·K^{-1}],
u – Velocity of gas flow, [m/s],
$\dot{m}_g$ – Mass gas flow rate, [kg/s],
x – Axial distance from the pipe inlet *($=i\cdot\Delta x$, $i=0,1,2,3...M$)*, current coordinates, [m],
Δx – Mesh length, [m],
α_{cvu} – Heat transfer coefficient from gas to the material (pipe wall), [W·m^{-2} ·K^{-1}],
$\dot{q}_{gen}$ – Heat flow rate per unit volume, [J·s^{-1}·m^{-3}],
t – Time ($=n\cdot\Delta t$, $n=0,1,2,3...N$), [s],
Δt – Time step, [s],
$\dot{Q}_{cvu}$ – Heat transfer rate by convection from gas to the material (pipe wall), [J/s],
$\dot{Q}_{cvo}$ – Heat transfer rate by convection to the environment, [J/s],
$\dot{Q}_{rado}$ – Heat transfer rate by radiation, [J/s],
D_2 – Outer diameter of the exhaust pipe, [m], and
D_1 – Inner diameter of the exhaust pipe, [m].

2.2. Description of the catalyst model

In formulating the model of heat transfer in the catalyst during the cold start engine, the following assumptions were taken into account:

– Monolith channel with non-cylindrical shape is simulated like a cylindrical channel with equivalent inlet cross-sectional area,
– Heat that originates from exothermal reactions of particular components of exhaust gases is neglected since the catalyst is not active. The catalyst is considered to function as a converter,
– Heat transfer by radiation is significant only when temperatures are high,
– The loss of heat by convection (either natural or forced) into the environment,
– Uniform distribution of gas temperature and velocity at the catalyst entry,
– Laminar gas flow in the monolith channels,
– Conduction and radiation are negligible in gas phase in comparison to convection,
– Catalyst material properties do not change significantly with temperature,
– Temperature and concentration of gas is identical for all catalyst channels, and

– Quasi-stationary assumptions can be applied.

Based on the aforementioned assumptions, calculation procedure for each time step is performed as follows:

1. Calculate temperature of the gas phase along the length of channels,
2. Calculate temperature of the catalyst body.

Gas phase

$$\frac{\partial T_{\mathrm{g}}}{\partial t}+u\frac{\partial T_{\mathrm{g}}}{\partial x}=\frac{-\delta\dot{Q}_{\mathrm{cvu}}}{\rho_{\mathrm{g}}\cdot\Delta V_g\cdot c_{\mathrm{pg}}}=-\frac{\alpha_{\mathrm{cvu}}\cdot O_{\mathrm{s}}\cdot\Delta x\cdot\left(T_{\mathrm{g}}-T_{\mathrm{mc}}\right)}{\rho_{\mathrm{g}}\cdot\Delta V_g\cdot c_{\mathrm{pg}}}$$
$$\frac{\partial T_{\mathrm{g}}}{\partial x}=-\frac{\alpha_{\mathrm{cvu}}\cdot O_s\cdot\left(T_{\mathrm{g}}-T_{\mathrm{mc}}\right)}{\rho_{\mathrm{g}}\cdot u\cdot{\Delta V_g}/{\Delta x}\cdot c_{\mathrm{pg}}}=-\frac{\alpha_{\mathrm{cvu}}\cdot O_s\cdot\left(T_{\mathrm{g}}-T_{\mathrm{mc}}\right)}{m_{\mathrm{g}}\cdot c_{\mathrm{pg}}} \tag{3}$$

The Catalyst Material

Since exothermal reactions in the catalyst are neglected during the cold start, equations of energy conservation are sufficient for the calculation (it is not necessary to consider mass transfer equations), *i. e.*:

$$\rho_{\mathrm{c}}\cdot c_{\mathrm{c}}\cdot\frac{\partial T_{\mathrm{mc}}}{\partial t}=\lambda_{\mathrm{c}}\cdot\left(\frac{\partial^2 T_{\mathrm{mc}}}{\partial x^2}\right)+\frac{\dot{Q}}{\Delta V_{\mathrm{mc}}},\qquad\frac{\partial T_{\mathrm{mc}}}{\partial t}=a_{\mathrm{c}}\left(\frac{\partial^2 T_{\mathrm{mc}}}{\partial x^2}\right)+\frac{\delta\dot{Q}}{\rho_{\mathrm{c}}\cdot c_{\mathrm{c}}\cdot\left(1-\varepsilon\right)\cdot\Delta V_{\mathrm{o}}}$$
$$\frac{\partial T_{\mathrm{mc}}}{\partial t}=a_{\mathrm{c}}\frac{\partial^2 T_{\mathrm{mc}}}{\partial x^2}+\frac{\delta\dot{Q}_{\mathrm{cvu}}-\delta\dot{Q}_{\mathrm{cvo}}-\delta\dot{Q}_{\mathrm{rado}}}{\rho_{\mathrm{c}}\cdot c_{\mathrm{c}}\cdot\Delta V_{mc}} \tag{4}$$
$$\delta Q=\delta Q_{cvu}-\delta Q_{cvo}=\alpha_{\mathrm{cvu}}\cdot O_{\mathrm{s}}\cdot\Delta x\cdot(T_{\mathrm{g}}-T_{\mathrm{mc}})-\alpha_{\mathrm{cvo}}\cdot O_o\cdot\Delta x\cdot(T_{mc}-T_{\mathrm{o}})$$

where:

α_{cvu} – Heat transfer coefficient from gas to the catalyst channel, [W·m^{-2}·K^{-1}],
T_{g} – Gas temperature in the catalyst channel, [K],
T_{mc} – Catalyst temperature, [K],
S_{o} – Surface area of cross section of the catalyst, [m^2],
ΔV_{o} – Geometrical control volume of the catalyst (=$S_{\mathrm{o}}\cdot\Delta x$), [m^3],
ε – Catalyst porosity [-],
ΔV_{g} – Infinitesimal control volume of gas (=$\varepsilon\cdot\Delta V_{\mathrm{o}}$), [m^3],
ΔV_{mc} – Infinitesimal control volume of catalyst material (=(1-ε)·ΔV_{o}), [m^3],
ρ_{c} – Mass density of the catalyst, [kg/m^3],
c_{c} – Specific heat of the catalyst, [J·kg^{-1}·K^{-1}],
λ_{c} – Thermal conductivity of the catalyst, [W·m^{-1}·K^{-1}],
a_{c} – Thermal diffusivity of the catalyst, (=$\lambda_{\mathrm{c}}/\rho_{\mathrm{c}}/c_{\mathrm{c}}$), [m^2·s^{-1}],
α_{cvo} – Heat transfer coefficient from the catalyst into the environment, [W·m^{-2}·K^{-1}],
O_{o} – Circumference of the outer shell in the cross section of the catalyst, [m], and
O_{s} – Total circumference of all catalyst channels in the cross section of the catalyst, [m].

Heat flux, ($\delta\dot{Q}$) includes: heat transfer rate by convection from gas to the catalyst, heat transfer rate by electric heating of the catalyst (if exists), heat transfer rate by convection into the

environment. As mentioned before, the heat that results from exothermal reactions, the heat transfer rate by radiation to the catalyst shell and from the shell into the environment are neglected.

2.3. Solution of the differential equations for the catalyst model case

Differential equations of heat transfer are solved using the finite difference method.

The changes in temperature and concentration of gas in the pipe and the catalyst during a period of time are taken as a series of quasi-stationary states.

Initial conditions are:

$t=0 \qquad 0 \le x \le L=M\cdot\Delta x \qquad T_{mc}(x,0)=T_{mcs}$ (5)

Boundary conditions are:

$x=0 \qquad 0 \le t \le N\cdot\Delta t \qquad T_g(0,t)=T_{gi}$ (6)

Since the conduction of heat through the monolith is considerably higher than convection on the front and rear monolith surfaces, the heat flux is neglected on the front and rear monolith surfaces *i. e.*:

$$\frac{\partial T_{mc}}{\partial x}\Big|_{x=0} = 0 \quad \Rightarrow \quad {T_{mc,0}}^{n} = {T_{mc,1}}^{n} \tag{7}$$

$$\frac{\partial T_{mc}}{\partial x}\Big|_{x=L} = 0 \quad \Rightarrow \quad {T_{mc,i}}^{n} = {T_{mc,i+1}}^{n}, \quad i = M \tag{8}$$

With the known initial conditions, eq. (5), the catalyst temperature in the first iteration step is known, then T_g is calculated from the equation for energy conservation eq. (3), together with the boundary conditions (6), using local analytical solution [7].

$$ {T_{g,i}}^{n} = {T_{mc,i}}^{n} + ({T_{g,i-1}}^{n} - {T_{mc,i}}^{n})e^{-NTU} \tag{9}$$

$$NTU = \frac{\alpha_{cvu}\Delta F}{\dot{m}_g c_{pg}} \tag{10}$$

where ΔF [m^2] is surface area of the catalyst segment through which heat is exchanged.

From eq. (4) and under boundary and initial conditions given by eqs. (5), (7) and (8), the catalyst temperature T_{mc} is calculated in a point of time and along the channel length by application of the finite difference method. Approximation of time derivative by finite differences is done by applying backwards difference, whereas the approximation of second derivatives by space is done by using central difference [7].

Discrete form of eq. (4) is as follows:

$$T_{mc,i}^{n} = T_{mc,i}^{n-1} + {a_{c,i}}^{n-1}\frac{\Delta t}{\Delta x^2}(T_{mc,i+1}^{n-1} - 2T_{mc,i}^{n-1} + T_{mc,i-1}^{n-1}) + \frac{\delta\dot{Q}_{cvu} - \delta\dot{Q}_{cvo}}{\rho_c \cdot c_c \cdot (1-\varepsilon)\cdot \Delta V_o}\Delta t\Big|_{i}^{n-1} \tag{11}$$

Stability criteria

For hyperbolic equations:

$$C = u\frac{\Delta t}{\Delta x} \leq 1 \tag{12}$$

For parabolic equations:

$$d = a_c \frac{\Delta t}{(\Delta x)^2} \leq \frac{1}{2} \tag{13}$$

Where:

C – *Courant* number, [-],

d – Diffusion number, [-].

a_c – Thermal diffusivity of the catalyst, ($=\lambda_c/\rho_c/c_c$), [$m^2 \cdot s^{-1}$].

Based on the above outlined mathematical model for engine exhaust pipes and the catalyst, "TERMO" computer programme was developed for calculation of unsteady heat transfer in the engine exhaust system [7].

Gas temperature at the exhaust system entry (limit condition) is assumed to be constant or defined by second-degree polynomials in terms of time. Optionally, the programme can accept measured gas temperature values at the engine exit or the values obtained by calculation, using the appropriate programme for engine operating cycle calculation.

Since the calculations for the catalyst and the pipes differ, the programme contains the option to decide interactively, for each calculated part, whether it is about the pipe or the catalyst. Based on the choice made, the sub-programme is automatically started for the appropriate calculation (the pipe or the catalyst). The programme also contains the possibility for taking into consideration radiation during the calculation process.

Input data are entered through the two files. The file *pipes.dat* contains dimensional and physical properties of materials data of the exhaust pipes and of the catalyst. The file *engine.dat* contains the dimensions of the engine and data of the working regime. There are the environmental temperature and the temperature of exhaust gases in this file, also.

The obtained output databases are gas temperatures in the selected part (*Tgas.dat*), material temperatures (*Tmat.dat*) in the selected part, mean temperature of the material part (*Tmid.dat*) and the input data and heat balance database (*pod.dat*). If the configuration includes double wall and insulated pipe, databases regarding temperature change of the external pipe (*Tmout.dat*) and insulation (*Tins.dat*) are also obtained.

3. Experimental method

Experimental investigations are conducted at the Faculty of Mechanical Engineering Kragujevac, Laboratory for IC engines. Two measurement installations were developed, the first one being intended for the model verification of the exhaust pipe and the second for the verification of the model of the catalyst. The measurement installations are shown in fig. 1.

The measuring installation must provide for constant gas flow and constant gas temperature at the inlet to the measuring pipe or the catalyst in order to use it for the model verification. The gas (working fluid) was air supplied by a compressor plant. Pressure in the installation was stable at 0.68 MPa. The pressure regulator (9) is placed at the installation entry to avoid pressure oscillations and to maintain constant pressure.

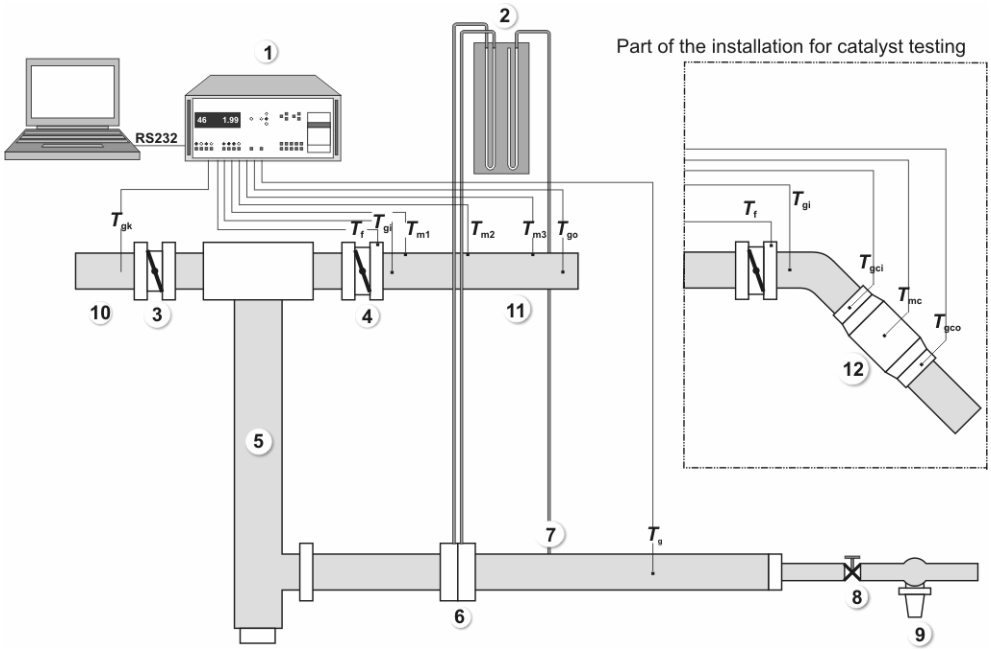

(1) – Measuring device HBM-UPM-60, (2) – Water column manometers, (3) – Valve on the control pipe, (4) – Valve on the measuring pipe, (5) – Heater, (6) – Orifice plate, (7) – Connection with the water manometer, (8) – Valve, (9) – Pressure regulator, (10) – Control pipe, (11) – Measuring pipe, (12) – Catalyst, T_{gk} *– Gas temperature in the control pipe,* T_f *– Flange temperature,* T_{gi} *– Gas temperature at the measuring pipe inlet (sensor position),* T_{gci} *– Gas temperature at the catalyst inlet,* T_{m1} *– Measuring pipe temperature at the beginning,* T_{m2} *– Measuring pipe temperature in the middle,* T_{m3} *– Measuring pipe temperature at the end,* T_{go} *– Gas temperature at the measuring pipe outlet,* T_{gco} *– Gas temperature at the catalyst outlet,* T_{mc} *– Catalyst temperature,* T_g *– Gas temperature upstream of the orifice plate.*

Figure 1 - Measurement installations

Investigations are conducted for different gas flow rates. The gas flow rate was controlled by the valve, (8). The gas flow rate is measured by an orifice plate with the nominal diameter of 10 mm, and pressure difference was read off a water column manometer.

The electric heater (5) CHROMALOX (1.5 kW) was used for heating the gas.

The gas passes through the control pipe (10) until the stationary gas temperature is reached. After the stationary gas temperature has been reached, gas flow is redirected into the measuring pipe (11) or the catalyst (12) and the control pipe is closed. Simultaneous closing of the control pipe and opening of the measuring pipe is done by throttle valves (3 and 4). Carburettor throttles are used as valves to prevent the gas leakage.

The measuring pipe is made of carbon steel. Gas temperature sensors and the pipe wall temperature sensors were placed on it. The second measurement installation consists of pipes made of stainless steel and the catalyst with metal carrier. Gas temperatures (before and after catalyst) and the catalyst material temperatures were measured also, fig. 2. In order to set proper boundary conditions for the model, it was necessary to measure the flange temperature. The flange connects the measuring pipe with the preceding part of the measurement installation.

The following values were measured in the above described measurement installations:

1. Gas flow rate through the measurement installation.

2. Environmental temperature and pressure.
3. Gas temperature and pressure upstream of the orifice plate. and
4. Gas and wall pipe temperatures.

3.1. Gas flow rate measurement

Volume gas flow rate measurement through the measurement installation is performed by means of an orifice plate with diameter 10 mm and water column manometer (2). Mass gas flow rate is calculated on the basis of measured data of the volume gas flow rate, environmental temperature and pressure. Calculated mass gas flow rate is corrected for gas temperature and pressure upstream of the orifice plate [8].

3.2. Environmental temperature and pressure measurement

Environmental temperature is measured by a thermocouple type K (Ni-Cr-Ni) suitable for an operating range from -30 to +1200 °C.

Environmental pressure is measured by mercury barometer (Torricelli's tube) with 0.1 mbar accuracy of reading.

3.3. Gas temperature and pressure upstream of the orifice plate

Thermocouple type K (Ni-Cr-Ni), with an operating range from -30 to +1200 °C is used for measuring gas temperature upstream of the orifice plate.

Gas pressure upstream of the orifice plate and differential pressure at the orifice plate are measured by water column manometers.

3.4. Temperature of gas, pipe wall and metallic catalyst carrier measurement

Thermocouples type K (Ni-Cr-Ni), with an operating range from -30 to +1200 °C, are used for measuring temperatures of the flange and on the metallic catalyst carrier.

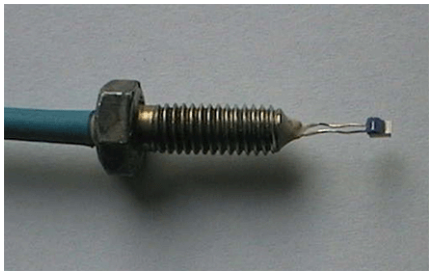

a) Adapted sensor screw for measuring temperatures of the gas in the pipe

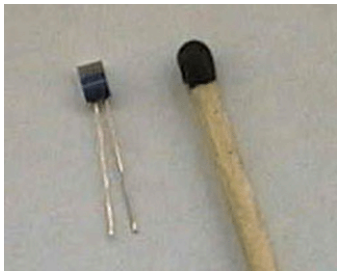

b) Size of the sensor compared to the wooden match stick

Figure 2 - PT100 sensors

Temperatures of the gas and the measuring pipe wall are measured by resistance sensors PT 100 – 2x2.3 mm, produced by Automation Products, RS. PT 100 sensors have small dimensions, small thermal inertia (thermal response 0.1 s) and are suitable for temperature operating range from -50 to

+250 ºC. Construction of PT 100 sensors is delicate and has to be adapted for measuring the gas temperature in the measuring pipe. Adapted temperature sensor intended for measuring the gas temperature in the pipe is shown in fig. 2a. The size of the sensor is compared with the size of a wooden match stick in fig. 2b.

PT 100 sensors are placed on the previously prepared pipe wall. Sensors are pasted by glue X60 (HBM) having the following characteristics: good heat transfer coefficient and small specific thermal capacity. The glue can be used in environments with maximum temperatures of 200 °C, which is significantly lower than in the experimental research. Placement of sensors on the pipe and the catalyst is shown in fig. 3.

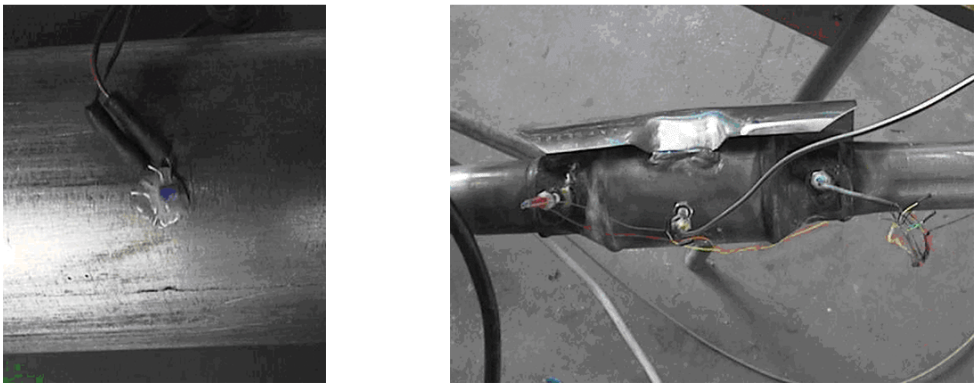

a) On the pipe (T_{m2}) b) On the catalyst (T_{gci}, T_{mc}, T_{gco})

Figure 3 - Measuring points and placement of sensors

Sensors are connected to the measuring device HBM-UPM-60 (1), fig. 1. The measuring device UPM is connected to a computer by means of an RS232 serial data interface. The appropriate software for communication between the device UPM and the computer and for data acquisition and storage was custom-written for this project.

4. Experimental research results and discussion

Measurements are conducted with different gas flow rates in the installation. After the gas temperature has become stationary for a given flow rate, the gas stream was passed through the measuring pipe or through the catalyst pipe (second installation). Temperatures of gas in pipe, temperatures of pipe material (catalyst carrier) at different positions and a flange temperature at inlet of measuring pipe are recorded. Environmental temperatures during measurements varied between 18 and 20 °C. Six measurements were conducted at the measurement installation with the pipe and five measurements were conducted with the catalyst. Three measurement results were then selected for the verification of the developed mathematical model.

Analyses of experimental results showed that:

1. The gas flow rate in a given measurement was constant over a period of time,
2. The constant gas temperature at the inlet of measuring pipe was not completely achieved,
3. Pipe wall temperatures increased significantly in the first 150-200 s, and
4. Temperature gradient in the catalyst carrier had a high value in the first 50-70 s.

During the above mentioned experiments, two conditions were to be achieved: the constant gas flow and the constant gas temperature at the inlet of the measuring installation. The first condition

was achieved, but the constant gas temperature at the inlet in the measuring pipe was not achieved, as well as at the catalyst inlet, figs. 4 and 5. Although the gas temperature in the control pipe was stationary, after the measuring pipe was opened and the control pipe was closed, the gas temperature in the measuring pipe decreased. After that, the gas temperature in the measuring pipe showed an increasing trend in time, until it became stationary. Part of the gas internal energy is spent on warming up the parts between the throttle and the flange, as well as of the measuring pipe flange itself. Certain period of time is necessary to achieve constant temperature of all parts.

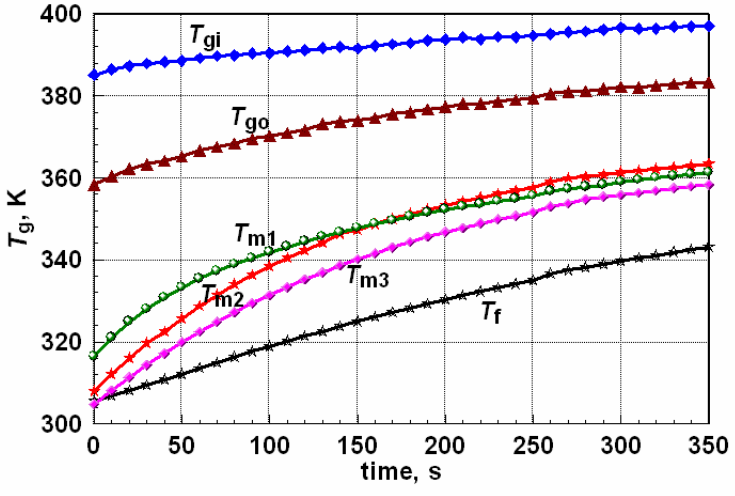

Figure 4 - Experimental results at the measuring pipe installation

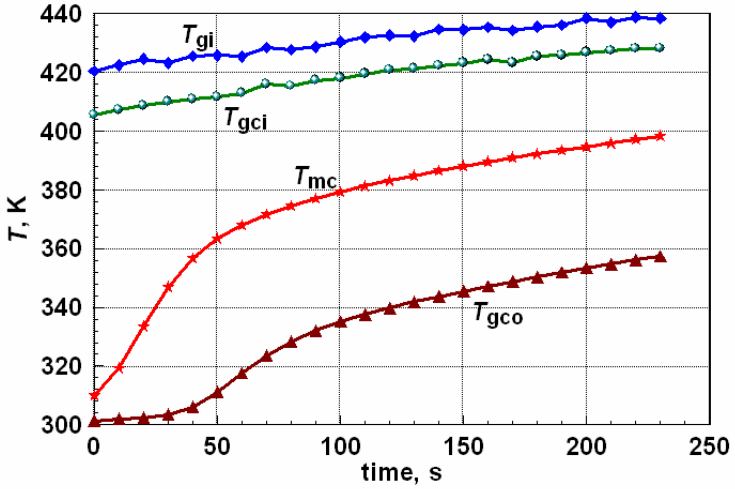

Figure 5 - Experimental results at the catalyst installation

Pipe wall temperatures increased in the first 150-200 s during all measurements. The measuring point at the beginning of the pipe (the first measuring point) is interesting for analysis. Above 200 s, the pipe wall temperature gradient decreases at the first measuring point (T_{m1}) while the pipe wall temperature at the second measuring point (T_{m2}) becomes higher than the pipe wall temperature at the first measuring point. This seems not to be logical at first sight because the gas temperature at the second measuring point is lower. At the second measuring point, with a similar heat transfer coefficient, heat transferred to the wall will be lower. In the vicinity of the first measuring point (at 18 mm distance) there is a flange, which represents a larger mass connected to the pipe wall. Temperature differences between the flange and the wall pipe increase during time as well as heat

conducted from the warmer pipe to the colder flange, because a larger mass is warming-up slowly. This observation is very significant. Firstly, it shows that the selection of boundary conditions for the present one-dimensional mathematical model, must take into consideration measured flange temperature which has significant influence on pipe heat balance. Secondly, in the modelling phase, it is important to consider parts with larger mass at pipeline. In that case, two-dimensional or three-dimensional models should be applied. Changes of the gas temperature at the pipe inlet and outlet, as well as the pipe wall temperatures and the flange temperature experimentally obtained with gas flow rate m=19 kg/h, are shown in fig. 4. Pipe wall temperatures were lower than the gas temperature at pipe outlet in all cases.

Gas temperatures measured at the inlet and the outlet of the catalyst pipe, as well as the material temperature change in the middle of the catalyst carrier for the gas flow rate m=7.3 kg/h are shown in fig. 5. Analysis of the catalyst temperature trend shows high temperature gradient in the first 50-70 second. After that, temperature increases slowly, almost linearly. Higher temperature gradient is observed under higher gas flow rate. The gas temperatures change at the outlet follows the catalyst carrier temperature change. The highest gas temperature gradient change is noticed in the first 50-70 s. Such temperature changes in the first period of time are logical, because heat conducted to the catalyst is the highest, with respect to large catalyst area responsible for convective heat transfer from gas and large temperature difference between gas and catalyst. It should be emphasized that the metallic catalyst carrier made of a very thin sheet (thickness of 0.1-0.15 mm) was used, which has small mass and low heat capacity and large area of convective heat exchange with gases. That is why the gas temperature at the catalyst outlet is lower than the catalyst carrier temperature in the middle of catalyst.

5. Verification of mathematical models and discussion

5.1. Verification of the exhaust pipe model

Setting the boundary conditions, of the mathematical model, means that the gas temperature and the pipe wall temperatures were defined for the same cross-sectional area (usually the pipe inlet). The first idea was to verify the model with the experimental results obtained with the simple pipe. In that case, the pipe inlet (pipe start) was represented by the measuring point of the first gas temperature sensor, and the pipe outlet was represented by the measuring point of the second gas temperature sensor. Experimental results showed that the influence of the flange heat capacity on the pipe wall temperature, at the position of the first pipe wall temperature sensor, is significant. It was the reason why the first idea about identical positioning of the pipe inlet and of the first gas temperature sensor was not correct.

In order to make the one-dimensional model results comparable with experiment, it is necessary to assume that the pipe starts from the flange, and include the flange effects in the model by the experimentally determined flange temperatures and heat conduction from the pipe to the flange.

The mathematical model is also modified in order to include calculation of the gas temperature and the pipe wall temperature backwards (from the first gas temperature sensor position to the flange position). Gas temperature boundary condition is determined by a polynomial expression obtained by an approximation of the measured gas temperature values at the first gas temperature

sensor position (at 18 mm distance from the flange). By way of backward calculation, from the first gas temperature sensor position to the position of the pipe inlet (the flange), gas temperature at the pipe inlet is determined. Calculated gas temperatures at the flange and measured flange temperature are approximated by polynomial expressions and are taken into calculation as boundary condition in the model verification process, fig. 6.

Linear approximation of the flange temperature measuring results yields $T_f=0.1\cdot t+306.8$; [K]. Gas temperature at the pipe inlet (flange position) can be approximated, with sufficient accuracy, by a linear equation: $T_{gi0}=0.23\cdot t+420$; [K], where "t" is time in seconds, fig. 6.

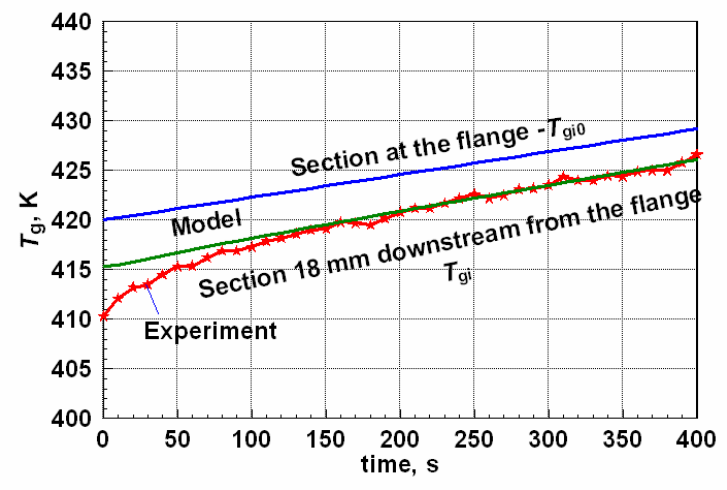

Figure 6 - Gas temperature at the measuring pipe inlet (section at the flange) and at position of the first gas temperature sensor (the gas flow rate in pipe was 9 kg/h)

Verification of the mathematical model is performed by comparing the measured gas temperatures, pipe wall temperatures (*i. e.* the catalyst carrier temperature at certain locations) to the calculated temperatures values.

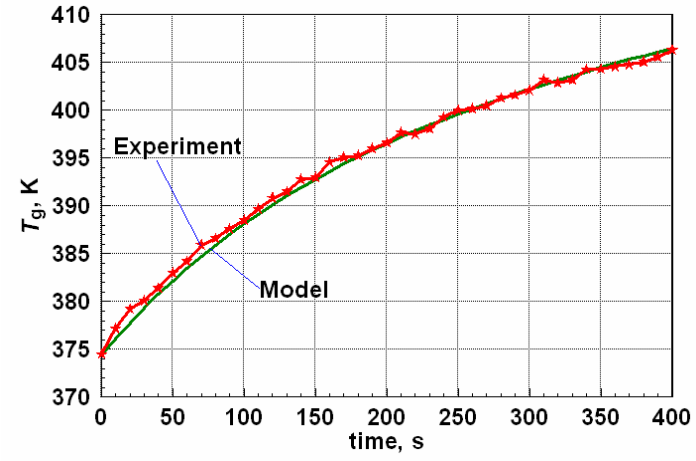

Figure 7 - Gas temperature at the measuring pipe outlet

Gas temperatures are measured at two positions and pipe temperatures are measured at three positions, shown in fig. 1, and are used in the model verification process.

The gas temperatures at the measuring pipe outlet obtained experimentally and by modelling are plotted in fig. 7.

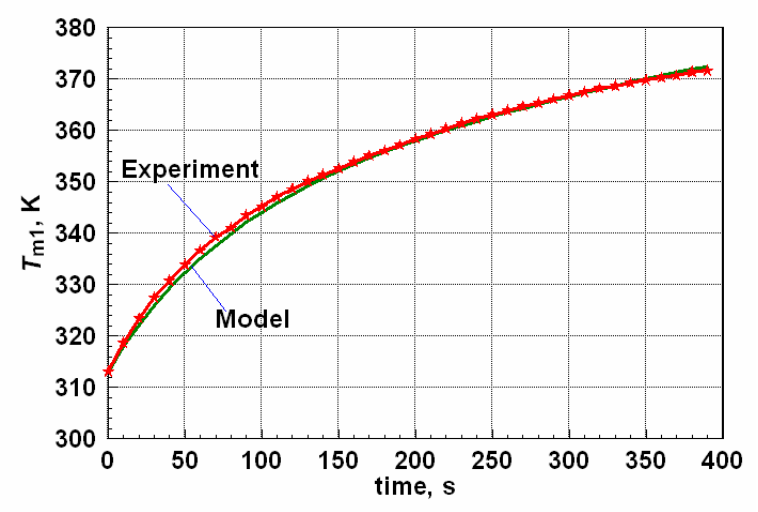

Figure 8 - Pipe wall temperature at the measuring point 1 (at the pipe inlet)

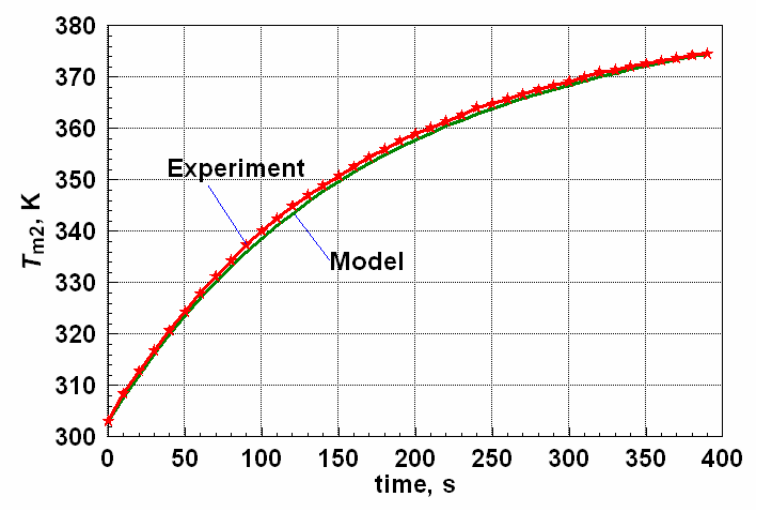

Figure 9 - Pipe wall temperature at the measuring point 2 (in the middle pipe)

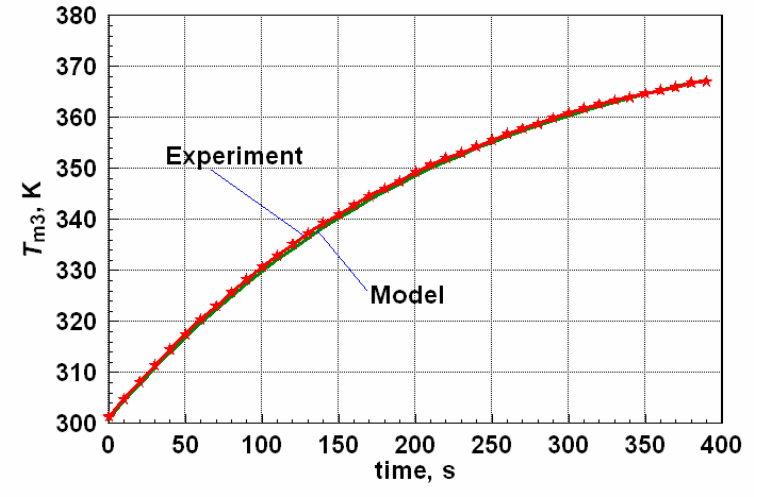

Figure 10 - Pipe wall temperature at the measuring point 3 (at the pipe outlet)

Pipe wall temperatures are shown in figs. 8, 9 and 10. All results are obtained for the same measurement and modelling conditions as in fig. 6.

Comparison between modelling and experimental results showed good agreement in all cases. This proves the model correctness and indicates its applicability for the optimization of the exhaust system design.

5.2. Verification of the catalyst model

Two measurement results (No 2 and No 3) are used for the catalyst model verification. Approximation functions of the measured gas temperature at catalyst inlet served as the model input data. Gas flow rates and functions of the gas temperature at the catalyst inlet for individual measurements are given in Table 1.

Table 1- Mass flow rates and gas temperatures in catalyst inlet

No	File name	Gas flow rate (kg/h)	Functions of gas temperature at catalyst inlet [K]
2	Kata 7	7.3	T_{gci}=407.5+0.0994·t
3	Kata 8	17.3	T_{gci}=386.8+0.0804·t

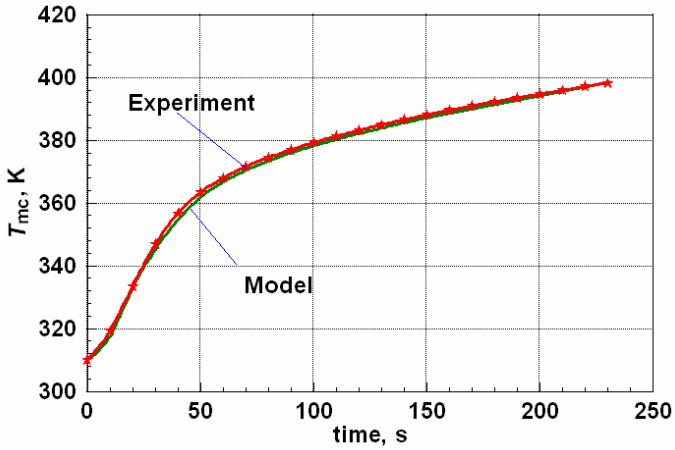

Figure 11 - Catalyst carrier temperatures (Kata 7)

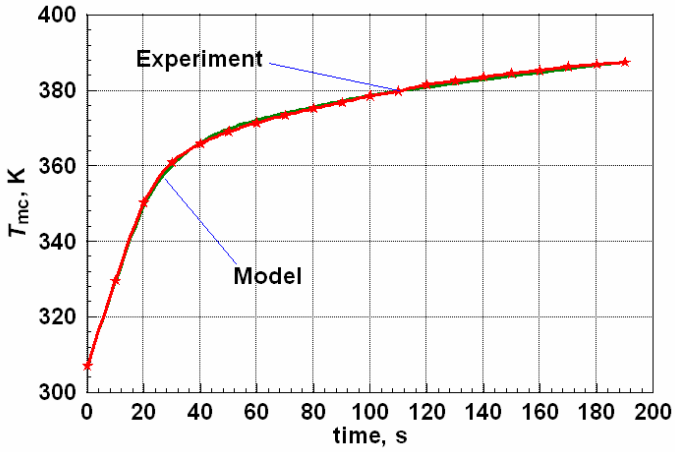

Figure 12 - Catalyst carrier temperatures (Kata 8)

Comparisons between measured and modelled catalyst temperatures at the mid-point of the catalyst carrier are given in figs. 11 and 12.

6. Conclusions

Large number of the exhaust system design parameters demand application of mathematical models and computers in the design phase. Model application reduces effort and time and production costs. Each developed model has to be verified experimentally.

If the exhaust piping consists of massive parts (like flanges), they should be taken into consideration in the model development phase. In this case, one-dimensional model does not give reliable results and three- or two-dimensional models should be applied. For the application of one-dimensional models, it is necessary to include the flange effects in the model by the experimentally determined flange temperatures and heat conduction from the pipe to the flange.

Good agreement between the modelling results and experimental data shows that the developed model and software can be successfully applied to different calculations of unsteady warmed-up exhaust systems.

Experimentally verified calculation method enables optimal exhaust system parameter selection both in the design and the improvement phases.

Nomenclature

a – Thermal diffusivity, ($\lambda/\rho/c$), [$m^2 \cdot s^{-1}$]
C – *Courant* number, ($= u\frac{\Delta t}{\Delta x} \le 1$), [–]
c_{pg} – Specific heat of the gas at constant pressure, [$J \cdot kg^{-1} \cdot K^{-1}$]
c – Specific heat, [$J \cdot kg^{-1} \cdot K^{-1}$]
d – Diffusion number, [–]
D – Diameter of the pipe, [m]
L – Length of pipe, [m]
$\dot{m}_g$ – Mass gas flow rate, [kg/s],
M – Number of time segments, [–]
N – Number of length segments, [–]
$\dot{Q}$ – Heat flux, [J/s]
O_s – Total circumference of all catalyst channels in the cross section of the catalyst, [m]
O_o – Circumference of the outer shell in the cross section of the catalyst, [m]
S_o – Surface area of cross section of the catalyst, [m^2]
t – Time, [s]
T – Temperature, [K]
u – Velocity of fluid flow, [m/s]

Greek letters

α – Heat transfer coefficient, [$W \cdot m^{-2} \cdot K^{-1}$]
λ – Thermal conductivity, [$W \cdot m^{-1} \cdot K^{-1}$]
ρ – Density, [kg/m^3]
ε – Catalyst porosity, [–]
Δt – Time step, [s]
Δx – Mesh length, [m]

Subscript

cvu – From gas to the material
cvo – From the catalyst into the environment
f – Flange
g – Gas
c – Catalyst
gi – Gas inlet
k – End
m – Material of pipe
mc – Material of catalyst
m_1 – At the beginning pipe
m_2 – On the middle pipe
m_3 – At the end pipe

p – Beginning
pg – Gas at constant pressure

Abbreviations

CSP - Cold Start Phase,
HC - Hydro Carbon,
CO - Carbon Oxide, and
NO - Nitrogen Oxide.

Acknowledgments

The paper is the result of the research within the project TR 35041 financed by the Ministry of Science and Technological Development of the Republic of Serbia.

References

[1] Laurikko J., Exhaust emissions performance of in-use TWC cars at low ambient temperatures, *Proceedings on CD*, 25th World Automotive Congress FISITA 1998, Paris, France, 1998, pp. F98P090.
[2] Petrović S., Kuzmanović M., Popović V., The Control of passengers' cars exhausts emissions, *Mobility &Vehicle Mechanics, Vol 20*, (1994). pp. 8-15.
[3] Marsh P., Acke F., KoniecznyR., Brück R., Hirth P., Application Guideline to Define a Catalyst Layout for Maximum Catalytic Efficiency, *SAE Paper 2001-01-0929*, (2001).
[4] Zu, Y., *et al*.: Cold Start Characteristics Study Based on Real Time NO Emissions in an LPG SI engine, *Thermal science*: Year 2010, Vol. 14, No. 4, pp. 937-942.
[5] Petrović V., Particulate matters from Diesel engine exhaust emission, *Thermal science*: Year 2008, Vol. 12, No. 2, pp. 183-198.
[6] Petković S., Pešić R., Lukić J., Heat transfer in exhaust system of a cold start engine at low environmental temperature, *Thermal Science: Year 2010*, vol. 14 (2010), No. Suppl., pp. 219-232.
[7] Petković S., Optimization of engine exhaust systems at low operating temperatures, (in Serbian) *Ph. D. Thesis*, Faculty of Mechanical Engineering, Banja Luka, Republic of Srpska, 2002.
[8] Pešić R., Davinić A., Petković S. and Taranović D., Volumetric efficiency- problems in experimental determination, *Proceedings*, (Radonjić D., Pešić R.) International Congress Motor Vehicles & Motors 2010, Kragujevac 7th-9th October 2010, pp. 442- 451.

Authors' affiliations:
Prof. Snežana Petković, Ph. D.
Faculty of Mechanical Engineering, Banja Luka, Bulevar Vojvode Stepe Stepanovića 75, Republic of Srpska

Prof. Radivoje Pešić, Ph. D., Prof. Jovanka Lukić, Ph. D.
Faculty of Mechanical Engineering in Kragujevac, Sestre Janjić 6, 34 000 Kragujevac, Serbia

Corresponding author: *Prof. Radivoje Pešić, Ph. D.*
E-mail: pesicr@kg.ac.rs